Perfectly Matched Feedback Control and Its Integrated Design for Multiaxis Motion Systems

Syh-Shiuh Yeh

Pau-Lo Hsu[1]
e-mail: plhsu@cc.nctu.edu.tw

Department of Electrical and Control Engineering,
National Chiao Tung University,
Hsinchu, 300 Taiwan

For motion systems with multiple axes, the approach of matched direct current gains has been generally adopted to improve contouring accuracy under low-speed operations. To achieve high-speed and high-precision motion in modern manufacturing, a perfectly matched feedback control (PMFBC) design for multiaxis motion systems is proposed in this paper. By applying stable pole-zero cancellation and including complementary zeros for uncancelled zeros for all axes, matched dynamic responses across the whole frequency range for all axes are achieved. Thus, contouring accuracy for multiaxis systems is guaranteed for the basic feedback loops. In real applications, the modeling error is unavoidable and the degradation and limitations of the model-based PMFBC exist. Therefore, a newly designed digital disturbance observer is proposed to be included in the proposed PMFBC structure for each axis to compensate for undesirable nonlinearity and disturbances to maintain the matched dynamics among all axes for the PMFBC design. Furthermore, the feedforward control loops zero phase error tracking controller are employed to reduce tracking errors. Experimental results on a three-axis CNC machining center indicate that both contouring accuracy and tracking accuracy are achieved by applying the present PMFBC design. [DOI: 10.1115/1.1789970]

1 Introduction

Generally, the performance of motion systems is dominated by both tracking and contouring accuracy, with appropriate feedback and feedforward control design for each axis. Poo et al. started the work of analyzing relations between feedback controllers and contouring errors [1]. Later, feedforward control loops were discussed in motion systems because they efficiently reduce the servo lags and passively decrease the contouring error [2–5]. In addition to well-designed feedback and feedforward control loops, the cross-coupled control (CCC) structure, which considers the mutual dynamic effects among all axes, was developed to reduce the contouring error by Koren [6]. Various improved CCC designs were then proposed [7–10]. Moreover, Lo proposed the transformation of the coordinates to obtain the moving basis to form a feedback controller for three-axis motion systems [10]. Chiu and Tomizuka [11] proposed a task-coordinated approach by considering all axes as first-order loops to obtain the feedback and the feedforward control loops. Cheng et al. [12] incorporated a zero phase error tracking controller (ZPETC) and a time-delay disturbance estimation scheme to cancel disturbances and potential nonlinearities, and to improve the overall system bandwidth for a single axis system. Yeh and Hsu [5,13] proposed the integrated control structure including the feedback, feedforward, and CCC to achieve the best tracking and contouring precision for multiaxis systems.

Although many advanced control algorithms and structures have been developed, the feedback controller design is still the most fundamental and crucial factor in obtaining desirable motion accuracy. To improve contouring accuracy in general multiaxis motion systems, feedback controllers should be designed to achieve matched dynamic characteristics among all axes. Although the design with direct current (dc) gains matched between two axes has been applied to systems under low-speed operations, such a design is not applicable to complex plants with usually higher-order models and under high-speed operations. In fact, a matched position control design in the whole frequency range is urgently needed for modern high-speed-high-precision manufacturing.

In this paper, the perfectly matched feedback control (PMFBC) is developed to achieve identical frequency responses for different axes by applying stable pole-zero cancellation and complementary zeros for uncancelled zeros among axes. Moreover, the present model-based design of PMFBC is sensitive to external disturbance and model uncertainty in real applications. Therefore, to ensure perfectly matched dynamic characteristics among all axes of multiaxis motion systems, the disturbance observer (DOB) was developed to reduce effects of the undesirable influence [14–16]. However, since problems of digital implementation based on the continuous-time DOB design exist, the digital disturbance observer (DDOB) structure is thus preferred. Since the discrete-time plant models may be nonminimum phase [17,18], a new design approach of DDOB is proposed in this paper for digital design and implementation. The filter Q, which contains three parts to deal with nonminimum phase nominal plants, includes: the stable pole-zero cancellations, all-pass filter, and a general low-pass filter in the DDOB design.

By applying the DDOB to the present PMFBC, the system models thus become more reliable and robust. Moreover, feedforward control for all axes is then included to further improve tracking accuracy. In the same time, the resultant contouring performance is significantly improved. Experimental results on a CNC machining center show that the perfectly matched feedback control achieves the desired matched dynamic properties among all axes. Moreover, the DDOB which significantly reduces the external disturbance effect is concluded to be required for implementing the PMFBC in practice.

2 PMFBC Design

To achieve matched dynamic responses in high frequency range for high-speed operations, theoretical derivation and design principles of PMFBC is introduced here. Consider the N-axis motion control system, as shown in Fig. 1. The corresponding nomenclature is as follows:

[1]To whom correspondence should be addressed.

Contributed by the Dynamic Systems, Measurement, and Control Division of THE AMERICAN SOCIETY OF MECHANICAL ENGINEERS for publication in the ASME JOURNAL OF DYNAMIC SYSTEMS, MEASUREMENT, AND CONTROL. Manuscript received by the ASME Dynamic Systems and Control Division December 18, 2002. Associate Editor: J. Tu.

Copyright © 2004 by ASME

Downloaded From: http://dynamicsystems.asmedigitalcollection.asme.org/ on 04/27/2014 Terms of Use: http://asme.org/terms

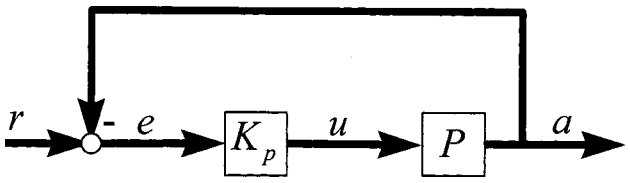

Fig. 1 The position feedback control systems

$r=[r_1\, r_2 \cdots r_n]^T$, r_i, $i=1,\cdots,n$: axial reference position command

$e=[e_1\, e_2 \cdots e_n]^T$, e_i, $i=1,\cdots,n$: axial position error

$u=[u_1\, u_2 \cdots u_n]^T$, u_i, $i=1,\cdots,n$: axial driving signal

$a=[a_1\, a_2 \cdots a_n]^T$, a_i, $i=1,\cdots,n$: actual axial position

$K_p=\text{diag}\{K_{p1},K_{p2},\cdots,K_{pn}\}$, K_{pi}, $i=1,\cdots,n$: position feedback controller of each axis

$P=\text{diag}\{P_1,P_2,\cdots,P_n\}$, P_i, $i=1,\cdots,n$: controlled plant of each axis

$T=\text{diag}\{T_1,T_2,\cdots,T_n\}$, T_i, $i=1,\cdots,n$: the position feedback system transfer function of each axis

The ith controlled axis $P_i(z^{-1})$ of the position loop is partitioned as follows:

$$P_i(z^{-1})=V_i(z^{-1})\cdot\frac{1}{1-z^{-1}}=\frac{z^{-1}\cdot B_i^{va}(z^{-1})\cdot B_i^{vu}(z^{-1})}{A_i^{v}(z^{-1})}\cdot\frac{1}{1-z^{-1}}$$

where

$V_i(z^{-1})$: the velocity loop

$A_i^{v}(z^{-1})$: polynomials of the velocity loop with all poles

$B_i^{va}(z^{-1})$: polynomials of the velocity loop with acceptable stable zeros

$B_i^{vu}(z^{-1})$: polynomials of the velocity loop with unacceptable zeros (unstable and nearly unstable zeros)

The position loop gain $L_i(z^{-1})$ of each axis is obtained as

$$L_i(z^{-1})=K_{pi}(z^{-1})\cdot P_i(z^{-1}) \tag{1}$$

As shown in Fig. 1 and Eq. (1), matching frequency responses of the closed-loop position system $T_i(z^{-1})$ implies that all the open-loop gains $L_i(z^{-1})$ are identical. To achieve matched frequency responses among all axes, the feedback controller $K_{pi}(z^{-1})$ corresponding to each axis is designed as

$$K_{pi}(z^{-1})=\alpha(z^{-1})\cdot\frac{A_i^{v}(z^{-1})}{B_i^{va}(z^{-1})}\cdot\prod_{\substack{j=1\\ j\neq i}}^{n}B_j^{vu}(z^{-1}) \tag{2}$$

Thus, the open-loop gain $L_i(z^{-1})$ becomes

$$L_i(z^{-1})=z^{-1}\cdot\alpha(z^{-1})\cdot\left(\prod_{j=1}^{n}B_j^{vu}(z^{-1})\right)\cdot\frac{1}{1-z^{-1}} \tag{3}$$

where $\alpha(z^{-1})$ is the controller with a design freedom embedded in the position feedback controller $K_{pi}(z^{-1})$ to achieve the desired stability and performance of the systems. $\Pi_{j=1,j\neq i}^{n}B_j^{vu}(z^{-1})$ is convolution of complementary zeros. By applying Eq. (3), the position feedback system transfer function of each axis $T_i(z^{-1})$ becomes

$$T_i(z^{-1})=\frac{L_i(z^{-1})}{1+L_i(z^{-1})} \tag{4}$$

Equation (4) shows that the transfer functions of all axes $T_i(z^{-1})$, $i=1,\cdots,n$ are identical and thus the dynamic characteristics among all axes are perfectly matched. Although the matched dynamic characteristics among all axes can be achieved by applying the present PMFBC as shown in Eq. (2), the order of controllers is unavoidably enlarged. In practice, it is preferable to reduce the order of controllers by adopting a lower-order model.

2.1 Design Example. To illustrate the proposed approach for perfectly matched design, feedback controllers are designed by applying the following velocity plants of a CNC machining center modeled as

$$V_x(z^{-1})=\frac{-0.0056z^{-1}+0.0421z^{-2}+0.1213z^{-3}+0.0922z^{-4}}{1-0.1087z^{-1}-0.3286z^{-2}-0.1708z^{-3}-0.1256z^{-4}+0.0228z^{-5}} \tag{5}$$

$$V_y(z^{-1})=\frac{-0.0015z^{-1}+0.0445z^{-2}+0.1251z^{-3}+0.0586z^{-4}}{1-0.236z^{-1}-0.3909z^{-2}-0.1736z^{-3}-0.1012z^{-4}+0.1616z^{-5}} \tag{6}$$

Three feedback controllers are designed as follows:

Case (i) mismatched design (mismatched). The proportional position controllers are designed to achieve a 0.707 damping ratio for each axis

$$K_{px}=0.07$$

$$K_{py}=0.1$$

Case (ii) dc gain matched design (matched dc gain). Feedback controllers are designed so that the position feedback loops are matched in the lower frequency range

$$K_{px}=0.07$$

$$K_{py}=0.0694$$

Case (iii) PMFBC. Feedback controllers are designed by applying the proposed method

$$\alpha=2.2\times10^{-5}$$

$$K_{px}=\frac{\begin{array}{l}2.2\times10^{-5}-6.742\times10^{-4}z^{-1}-1.383\times10^{-3}z^{-2}\\+3.744\times10^{-4}z^{-3}+5.88\times10^{-4}z^{-4}+3.323\times10^{-4}z^{-5}\\+1.666\times10^{-4}z^{-6}-3.301\times10^{-5}z^{-7}\end{array}}{-5.612\times10^{-3}}$$

$$K_{py}=\frac{\begin{array}{l}2.2\times10^{-5}-1.702\times10^{-4}z^{-1}-4.45\times10^{-4}z^{-2}\\-1.886\times10^{-4}z^{-3}+2.976\times10^{-4}z^{-4}+2.441\times10^{-4}z^{-5}\\+8.421\times10^{-5}z^{-6}-4.021\times10^{-5}z^{-7}-5.840\times10^{-5}z^{-8}\end{array}}{-1.486\times10^{-3}-8.904\times10^{-4}z^{-1}}$$

where α is simply chosen here to assure a suitable numerical order for the controlled axes. Frequency responses of cases (i)–(iii) are shown in Figs. 2–4, respectively. As shown in Fig. 2, the mismatched design yields the worst contouring performance. Figure 3 shows that the matched dc-gain design in case (ii) achieves similar dynamic properties in the low frequency range corresponding to the slow motion speed. Moreover, PMFBC as shown in Fig. 4

Downloaded From: http://dynamicsystems.asmedigitalcollection.asme.org/ on 04/27/2014 Terms of Use: http://asme.org/terms

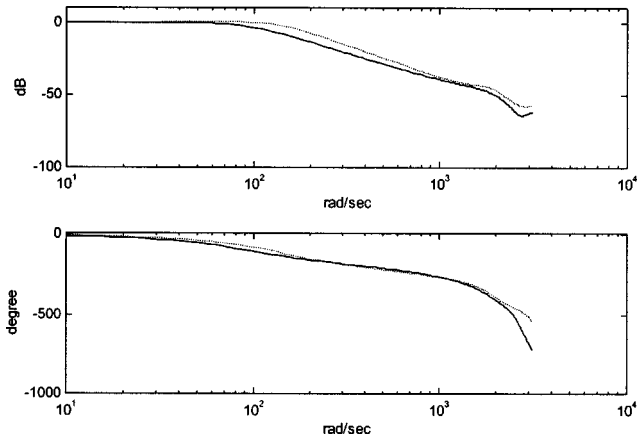

Fig. 2 Frequency responses of mismatched design, case (i) (solid: *X* axis; dashed: *Y* axis)

achieves identical frequency responses among all axes and thus provides the best contouring accuracy in all speed operations.

2.2 Model Reduction. Although motion precision can be improved by applying the proposed PMFBC controllers, the proposed design algorithms also generally lead to higher-order controllers. In practice, model reduction methods can be applied to the redundant modes of controlled plants. In this paper, we use

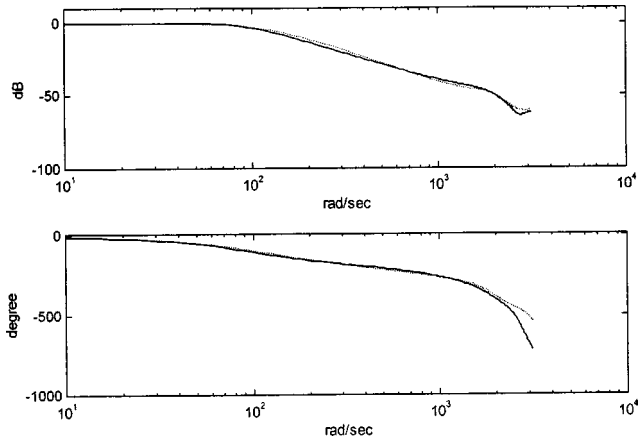

Fig. 3 Frequency responses of matched dc-gain design, case (ii) (solid: *X* axis; dashed: *Y* axis)

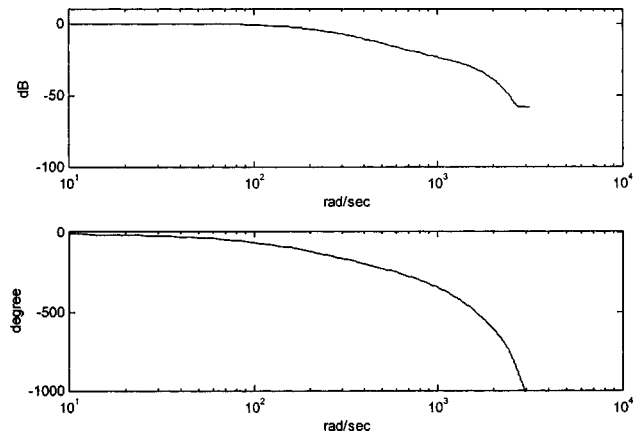

Fig. 4 Frequency responses of PMFBC, case (iii) (solid: *X* axis; dashed: *Y* axis)

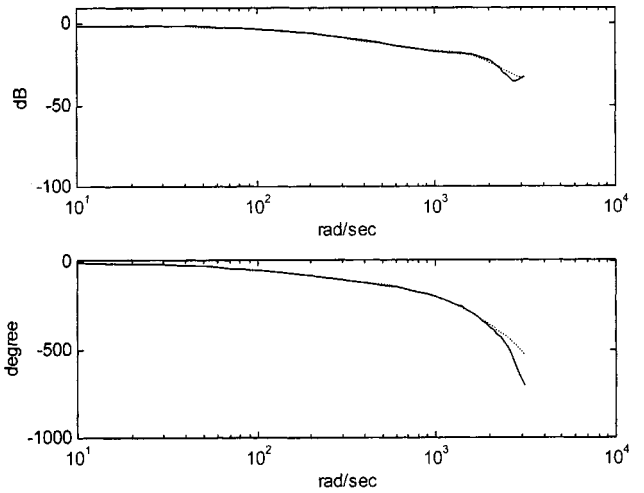

Fig. 5 Frequency responses of the original (solid) and the reduced order (dashed) plant

balanced realization to remove the least observable and controllable modes [19]. We thereby reduce the model of the velocity plant from fifth order to third order

$$V_x(z^{-1}) = \frac{-0.00437948z^{-1} + 0.04225802z^{-2} + 0.09618655z^{-3}}{1 - 0.88944678z^{-1} + 0.23980063z^{-2} - 0.19529895z^{-3}} \tag{7}$$

$$V_y(z^{-1}) = \frac{-0.00141126z^{-1} + 0.04402946z^{-2} + 0.09340968z^{-3}}{1 - 0.83356582z^{-1} - 0.04295967z^{-2} + 0.03239339z^{-3}} \tag{8}$$

The perfectly matched feedback controllers are designed as follows:

Case (iv) PMFBC with reduced-order plant model. Practical feedback controllers are designed by applying the proposed method and the reduced order model

$$\alpha = 2.2 \times 10^{-5}$$

$$K_{px} = \frac{2.2\times10^{-5} - 7.0594\times10^{-4}z^{-1} - 8.4038\times10^{-4}z^{-2} + 1.1262\times10^{-3}z^{-3} - 2.1513\times10^{-4}z^{-4} + 2.8438\times10^{-4}z^{-5}}{-4.3794\times10^{-3}}$$

$$K_{py} = \frac{2.2\times10^{-5} - 2.3061\times10^{-4}z^{-1} - 3.0718\times10^{-4}z^{-2} + 4.1259\times10^{-4}z^{-3} + 1.3881\times10^{-5}z^{-4} - 1.5652\times10^{-5}z^{-5}}{-1.4112\times10^{-3}}$$

The frequency responses of the original and the reduced-order plant in the *X* axis are shown in Fig. 5. Results indicate that the approximation is satisfactory up to 1000 rad/s. Also, as shown in Fig. 6, the frequency responses of the biaxial system are virtually matched up to the same frequency of around 1000 rad/s.

3 DDOB Design

Theoretically, the perfectly matched feedback control provides contouring accuracy because of the matched dynamic properties among all axes. In real applications, motion precision is easily degraded by external disturbances and model uncertainty. Although DOB was developed to degrade the external disturbance effects, its implementation on computer-controlled processes is not direct and approximation is required. Moreover, available DDOB [14–16] cannot be directly applied to nonminimum phase

Downloaded From: http://dynamicsystems.asmedigitalcollection.asme.org/ on 04/27/2014 Terms of Use: http://asme.org/terms

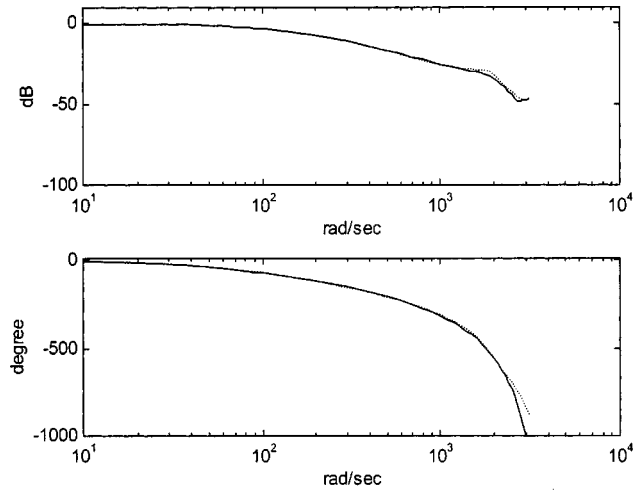

Fig. 6 Frequency responses of the PMFBC with the reduced-order plants

plant models which may exist in motion systems with discrete-time models [17,18]. Therefore, a newly developed DDOB with a simple finite impulse response disturbance estimator which can be applied to nonminimum phase motion systems is proposed in this paper, As the present PMFBC is implemented in real applications, the DDOB is required to compensate for the undesired nonlieairities, model uncertainties, and disturbances to maintain the matched dynamic responses for all axes.

Consider the new DDOB system as shown in Fig. 7, where

u, ϵ, ν: reference input, driving force and velocity output of controlled plant, respectively

d, $\hat{d}$: external disturbance and estimated disturbance, respectively

$\hat{\delta}$: feedback signal

ξ_ν: measured noise

$N(z^{-1})$, $D(z^{-1})$: numerator and denominator of plant, respectively

$N_d(z^{-1})$: structure of external disturbance

$N_n(z^{-1})$, $D_n(z^{-1})$: numerator and denominator of nominal plant, respectively

$Q(z^{-1})$: a low-pass filter

The velocity response of the controlled plant is derived as

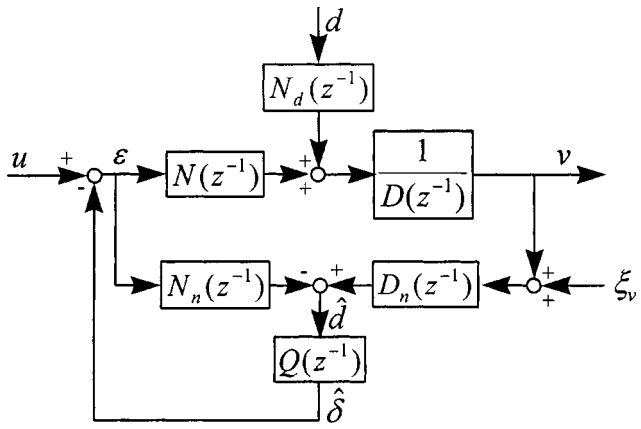

Fig. 7 The structure of the newly developed DDOB

$$\nu = \frac{N}{D(1-N_nQ)+ND_nQ}u + \frac{N_d(1-N_nQ)}{D(1-N_nQ)+ND_nQ}d - \frac{NQD_n}{D(1-N_nQ)+ND_nQ}\xi_\nu$$

$$= \frac{N}{D}\frac{1}{(1-N_nQ)+\frac{N}{D}D_nQ}u + \frac{N_d}{D}\frac{(1-N_nQ)}{(1-N_nQ)+\frac{N}{D}D_nQ}d - \frac{N}{D}\frac{D_nQ}{(1-N_nQ)+\frac{N}{D}D_nQ}\xi_\nu \tag{9}$$

If the filter Q is designed such that $N_n(z^{-1})Q(z^{-1})=1$, Eq. (9) becomes

$$\nu = \frac{N_n}{D_n}u - \xi_\nu$$

On the other hand, if the filter Q is designed such that $N_n(z^{-1})Q(z^{-1})=0$, Eq. (9) becomes

$$\nu = \frac{N}{D}u + \frac{N_d}{D}d$$

Therefore, the filter Q is designed as

$$\begin{cases} N_n(z^{-1})Q(z^{-1})=1, & \text{in the lower frequency region} \\ N_n(z^{-1})Q(z^{-1})=0, & \text{in the higher frequency region} \end{cases} \tag{10}$$

to degrade external disturbances and reject measurement noise. The design of the filter Q depends greatly on the nominal numerator $N_n(z^{-1})$. It contains the following three steps: (1) stable pole-zero cancellations, (2) an all-pass filter, and (3) an embedded low-pass filter.

To obtain the stable pole-zero cancellation, the nominal numerator $N_n(z^{-1})$ is separated

$$N_n(z^{-1}) = N_n^a(z^{-1})N_n^u(z^{-1})$$

where

$N_n^a(z^{-1})$: an acceptable polynomial with stable roots.

$N_n^u(z^{-1})$: an unacceptable polynomial with unstable and nearly unstable roots.

Suppose the unacceptable polynomial $N_n^u(z^{-1})$ is represented as

$$N_n^u(z^{-1}) = b_1z^{-1} + b_2z^{-2} + \cdots b_mz^{-m} = z^{-m}(b_1z^{m-1} + b_2z^{m-2} + \cdots b_m) = z^{-m}\cdot\hat{N}_n^u(z)$$

Then, design of the filter Q is

$$Q(z^{-1}) = \frac{1}{N_n^a(z^{-1})\cdot[\hat{N}_n^u(z)]^*}\cdot \mathrm{LPF}(z^{-1}) \tag{11}$$

where $[\cdot]^*$ denotes the complex conjugate operator and

$$[\hat{N}_n^u(z)]^* = (b_1z^{-(m-1)} + b_2z^{-(m-2)} + \cdots b_m) \tag{12}$$

Downloaded From: http://dynamicsystems.asmedigitalcollection.asme.org/ on 04/27/2014 Terms of Use: http://asme.org/terms

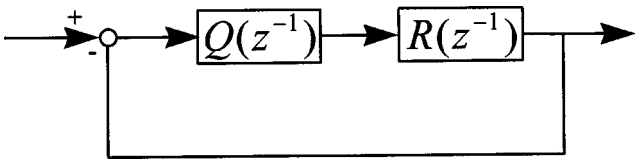

Fig. 8 The equivalent feedback loop system

Equation (12) is stable and realizable, and $\{N_n^u(z^{-1})/[\hat{N}_n^u(z)]^*\}$ forms a stable all-pass filter. The low-pass filter LPF(z^{-1}) can be designed such that

$$Q(z^{-1})\cdot N_n(z^{-1})=\frac{N_n^u(z^{-1})}{[\hat{N}_n^u(z)]^*}\cdot \mathrm{LPF}(z^{-1})$$

possesses the desired frequency response as given in Eq. (10).

The stability of the DDOB, as shown in Fig. 7, can be proved by the following lemma

3.1 Lemma. Define the equivalent plant R as

$$R=D_n\cdot\frac{N}{D}-N_n$$

and the equivalent feedback system S as shown in Fig. 8. Then, the DDOB as shown in Fig. 7 is internally stable if the equivalent feedback system S is internally stable.

Proof:

Since

(1) system S is internally stable implies that $Q(z^{-1})$, $R(z^{-1})$, and $[1/1+Q(z^{-1})R(z^{-1})]$ are all stable, and

(2) all subsystems of DDOB, $\{N_d, N, 1/D, N_n, D_n, Q\}$, are all stable, the DDOB is thus internally stable.

According to the lemma, system stability directly depends on the filter Q and thus the low-pass filter LPF(z^{-1}) in filter Q must be designed to achieve both desired stability and frequency responses. However, as shown in Eq. (9), if

$$N_n(z^{-1})=N(z^{-1}) \quad \text{and} \quad D_n(z^{-1})=D(z^{-1}),$$

the velocity response is

$$\nu=\frac{N}{D}u+\frac{N_d}{D}\frac{(1-NQ)}{1}d-\frac{NQ}{1}\xi_\nu,$$

and the stability is dominated by the denominator $D(z^{-1})$ and the filter $Q(z^{-1})$. It implies that the design of the filter $Q(z^{-1})$ does not affect the stability of the DDOB if the filter $Q(z^{-1})$ is stable. Furthermore, the equivalent plant R in Fig. 8 also shows that the design of filter Q may be invalid when the nominal plant model N_n/D_n is significantly different from the real plant N/D.

3.2 Design Example. The nominal plant N_n/D_n is chosen to be the reduced-order model of the velocity loop as shown in Eqs. (7)–(8). Therefore, the DDOB is designed as

Case (v) perfectly matched feedback control design with DDOB (PMFBC+DDOB). To achieve stable system he filter Q is designed as

$$Q_x(z^{-1})=\frac{\begin{array}{l}0.00497194+0.024859747z^{-1}\\+0.04971949z^{-2}+0.04971949z^{-3}\\+0.02485974z^{-4}+0.00497194z^{-5}\end{array}}{\begin{array}{l}1-2.94719898z^{-1}+3.23989221z^{-2}\\-1.20983151z^{-3}-0.4541163z^{-4}+0.52748002z^{-5}\\-0.14373367z^{-6}+0.00883831z^{-7}\end{array}}$$

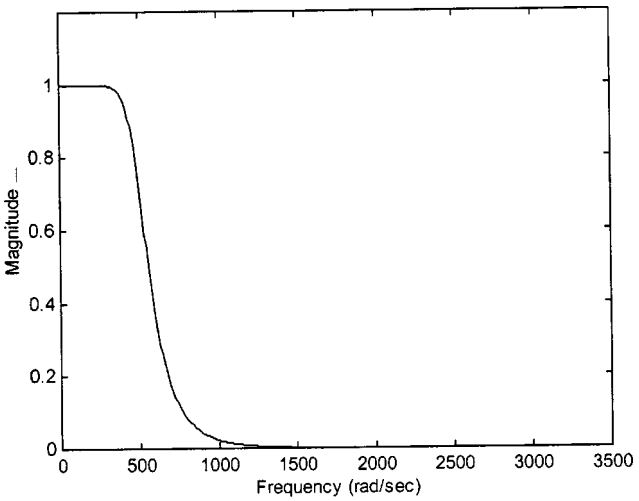

Fig. 9 The designed frequency response of $Q(z^{-1})N_n(z^{-1})$

$$Q_y(z^{-1})=\frac{\begin{array}{l}0.00511975+0.02559877z^{-1}+0.05119755z^{-2}\\+0.05119755z^{-3}+0.02559877z^{-4}+0.00511975z^{-5}\end{array}}{\begin{array}{l}1-2.91517429z^{-1}+3.16186245z^{-2}-1.1599981z^{-3}\\-0.41974012z^{-4}+0.46329684z^{-5}\\-0.11089379z^{-6}+0.00293275z^{-7}\end{array}}$$

Figure 9 shows the frequency response of $Q(z^{-1})N_n(z^{-1})$ for the X axis with a bandwidth of 500 rad/s which is suitable for the velocity loop around 100 Hz bandwidth.

4 The Feedforward Control Design

Although perfectly matched dynamic characteristics among all axes can be achieved by applying the PMFBC and the external disturbance can be significantly reduced by applying the DDOB to achieve improved the contouring accuracy, the servo lag effect should be minimized to improve the tracking accuracy of multi-axis motion systems. Therefore, the common feedforward controller for motion systems, the ZPETC proposed by Tomizuka can be suitably employed [2]. Consider the control systems with two degrees of freedom as shown in Fig. 10. The corresponding nomenclature is listed later

$r_f=[r_{f1}\, r_{f2}\cdots r_{fn}]^T$, r_{fi}, $i=1,\cdots,n$: the filtered axial reference position command

$F=\mathrm{diag}\{F_1,F_2,\cdots,F_n\}$, F_i, $i=1,\cdots,n$: the ZPETC designed feedforward control for each axis

Suppose the position feedback loop transfer function $T_i(z^{-1})$ is represented as

$$T_i(z^{-1})=\frac{a_i(z^{-1})}{r_{fi}(z^{-1})}=\frac{z^{-di}B_i(z^{-1})}{A_i(z^{-1})}=\frac{z^{-di}B_a^i(z^{-1})B_u^i(z^{-1})}{A_i(z^{-1})} \tag{13}$$

where

z^{-di}: di delay of ith axis position feedback loop

$A_i(z^{-1})$: denominator of ith axis position feedback loop

$B_i(z^{-1})$: numerator of ith axis position feedback loop

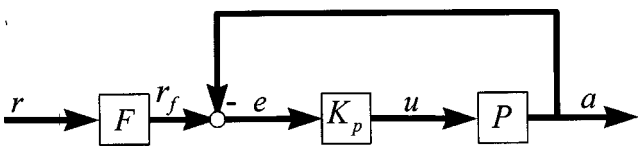

Fig. 10 The two degrees-of-freedom control system

Downloaded From: http://dynamicsystems.asmedigitalcollection.asme.org/ on 04/27/2014 Terms of Use: http://asme.org/terms

$B_a^i(z^{-1})$: polynomials with acceptable zeros

$B_u^i(z^{-1})$: polynomials with unacceptable zeros

Note that the optimal ZPETC [5] further improves tracking performance. The designed feedforward controller F_i is in the following form:

$$F_i(z^{-1}) = \left(\sum_{k=0}^{N-P} \alpha_k \cdot (z^k + z^{-k}) \right) \cdot \left(\frac{B_u^i(z)}{B_u^i(1)^2} \right) \cdot \left(\frac{z^{di} A_i(z^{-1})}{B_a^i(z^{-1})} \right) \tag{14}$$

Design Example. The hybrid structure which combines (*a*) perfectly matched feedback control, (*b*) the optimal ZPETC, and (*c*) the DDOB, is designed to improve both tracking and contouring accuracy in multi-axis motion systems. Because of model uncertainty in the higher frequency region, the bandwidth is chosen around 500 rad/s in design.

Case (vi) hybrid structure (hybrid). The feedforward controller is designed with optimal ZPETC [5] given as

$$F(z^{-1}) = \frac{\begin{array}{l} 0.99518942z^7 - 6.40810113z^6 + 18.04061216z^5 \\ -3.28244714z^4 - 11.2545723z^3 + 1.29958907z^2 \\ +1.11190473z^1 + 0.29919024 + 0.27312898z^{-1} \\ -0.07579595z^{-2} - 0.00750972z^{-3} + 0.00980315z^{-4} \\ -0.00101341z^{-5} + 0.00002189z^{-6} \end{array}}{1}$$

Figure 11 shows the frequency response of feedforward controlled system. The figure indicates that unity-gain region falls within [0, 785 rad/s]. The hybrid control is obtained by adding the feedforward controller F to the PMFBC+DDOB. Because the DDOB is designed under the frequency condition as shown in Eq. (10), the design of the optimal ZPETC depends heavily on the bandwidth of $Q(z^{-1})N_n(z^{-1})$. With the decrease in uncertainty obtained by applying the feedback control, the optimal ZPETC can be designed to make the unity gain region cover the bandwidth of $Q(z^{-1})N_n(z^{-1})$ as shown in Figs. 9 and 11.

Basically, the proposed design by integrating PMFBC, DDOB, and ZPETC are independent. The feedback loop of PMFBC for all axes should be designed in the first step. Then, the DDOB is designed for each axis so that the matched dynamic responses of PMFBC can be well maintained. Finally, the feedforward control ZPETC is directly included. Thus, not only both contouring and tracking accuracy can be improved by applying PMFBC and ZPETC, respectively, the proposed hybrid control structure is also robust because of the inclusion of DDOB.

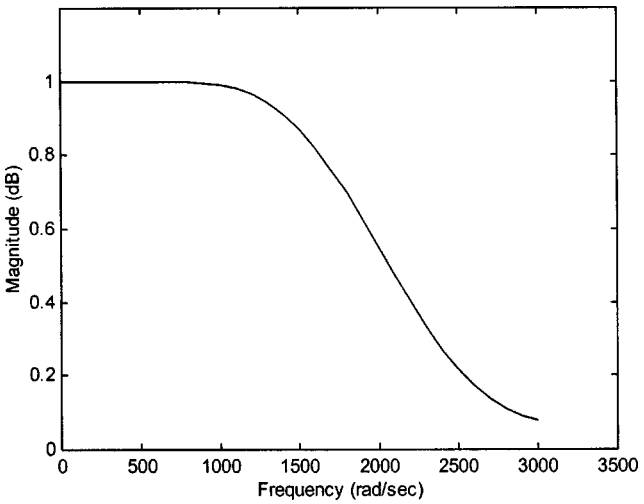

Fig. 11 The frequency response of the feedforward controlled system

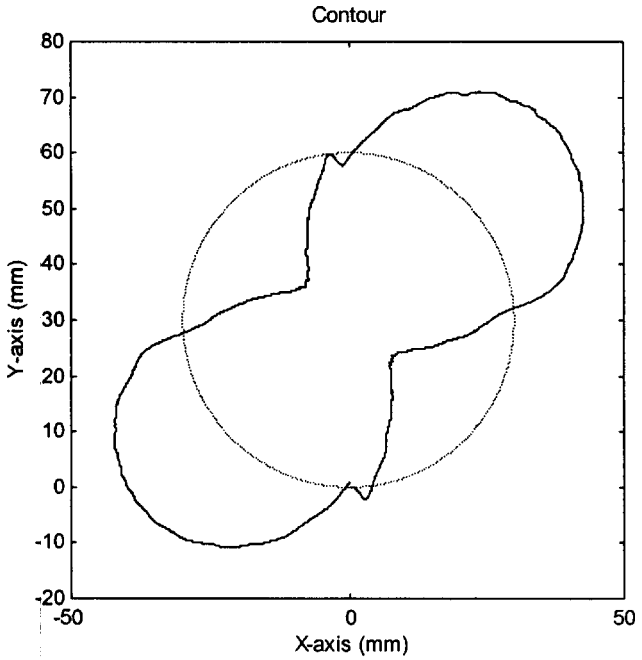

Fig. 12 Experimental results for design with mismatched gains case (i)

5 Experimental Results

5.1 Experimental Setup. The experimental setup of the DYNA 1007 CNC machining center is the same as in Ref. [20]. A PC-486 generated the main control commands and recorded the principle signals including: the input command calculation for different contours, the implementation of controller, and the control

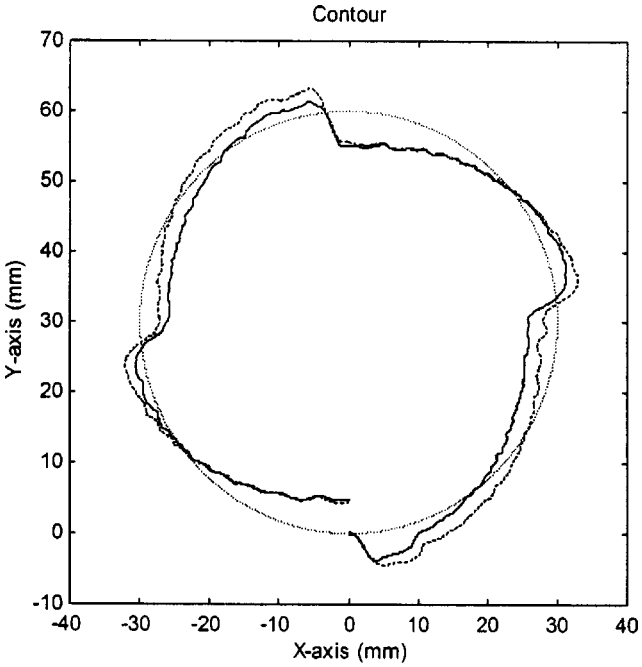

Fig. 13 Experimental results for matched dc-gain (case (ii), dashed) and PMFBC (case (iii), solid)

Downloaded From: http://dynamicsystems.asmedigitalcollection.asme.org/ on 04/27/2014 Terms of Use: http://asme.org/terms

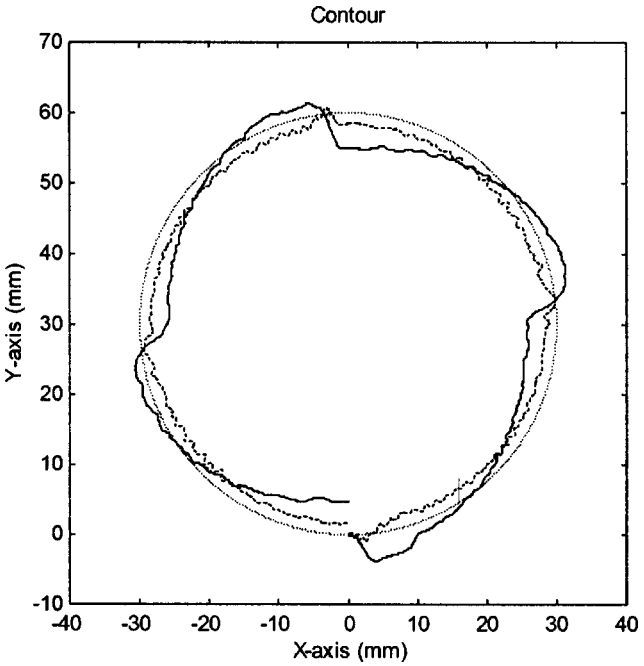

Fig. 14 Experimental results for PMFBC (case (iv), solid) and PMFBC+DDOB (case (v), dashed)

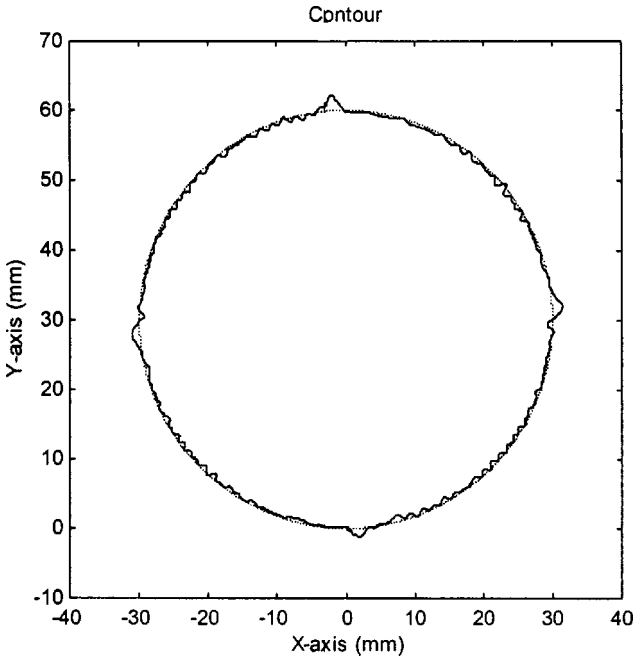

Fig. 15 Experimental results for PMFBC+DDOB+ZPETC (case (vi), solid)

Table 1 Experimental results with a high-speed circular com

Controller / Performance	Case (i) Mismatched	Case (ii) Matched DC gain	Case (iv) PMFBC	Case (v) PMFBC +DDOB	Case (vi) PMFBC +DDOB +ZPETC
Contouring error (RMS, *mm*)	0.131848	0.024243	0.024672	0.014465	0.004116
Tracking error (RMS, *mm*)	1.02469	1.20283	1.110041	1.174985	0.005239
Roundness (*mm*)	0.412357	0.098839	0.091662	0.035097	0.031962

Table 2 Experimental results with a low-speed circular com

Controller / Performance	Case (i) Mismatched	Case (ii) Matched DC gain	Case (iv) PMFBC	Case (v) PMFBC +DDOB	Case (vi) PMFBC +DDOB +ZPETC
Contouring error (RMS, *mm*)	0.031189	0.032109	0.029129	0.001581	0.0016
Tracking error (RMS, *mm*)	0.1724	0.204648	0.188983	0.152142	0.001869
Roundness (*mm*)	0.109846	0.143246	0.132729	0.018544	0.019013

Downloaded From: http://dynamicsystems.asmedigitalcollection.asme.org/ on 04/27/2014 Terms of Use: http://asme.org/terms

inputs to the velocity loop. The machine feed system is driven by scanning electron microscopy alternating current servo motors. The PC-486 interface utilized an AD/DA card to send and receive the control inputs and position outputs respectively at a sampling period of 1 ms.

A circular contour command with a radius of 30 mm and a linear contour command with a 45 deg incline angle were applied with a high speed of 5 m/min and a low speed of 600 mm/min. Note that 5 m/min is the highest speed of the DYNA CNC machining center, and that speeds of around 600 mm/min are common for fine machining process.

5.2 Results and Discussions. Experimental results for the different control structures under different speed operations as the command 5 and 0.6 m/min are shown in Figs. 12–15 and summarized in Tables 1 and 2, respectively. For linear commands with different speeds, tracking errors are shown in Fig. 16 and Tables 3 and 4. All experimental results indicate that both the matched dc-gains design and PMFBC design significantly reduces contouring error compared with the mismatched design as shown in Figs. 12 and 13. Furthermore, results for PMFBC and its integration with the DDOB and the ZPETC are normalized to the results for the matched dc-gains design as summarized in Figs. 17 and 18. The merits of the proposed control structure by integrating PMFBC, DDOB, and ZPETC can be clearly indicated as in Tables 1–4 as follows:

1. The proposed PMFBC design results in matched dynamic

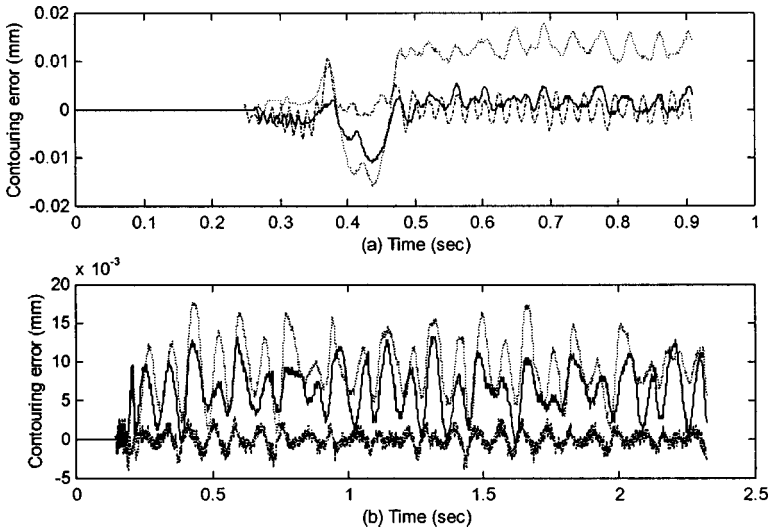

Fig. 16 Experimental results with linear commands (*a*) high speed, (*b*) low speed (solid: PMFBC, dashed: matched dc-gain, dashdot: PMFBC+DDOB +ZPETC)

Table 3 Experimental results with a high-speed linear com

Controller / Performance	Case (i) Mismatched	Case (ii) Matched DC gain	Case (iv) PMFBC	Case (v) PMFBC +DDOB	Case (vi) PMFBC +DDOB +ZPETC
Contouring error (RMS, *mm*)	0.145338	0.009627	0.002725	0.002107	0.001998
Tracking error (RMS, *mm*)	0.824483	0.963995	0.887487	0.93199	0.005302

Table 4 Experimental results with a low-speed linear com

Controller / Performance	Case (i) Mismatched	Case (ii) Matched DC gain	Case (iv) PMFBC	Case (v) PMFBC +DDOB	Case (vi) PMFBC +DDOB +ZPETC
Contouring error (RMS, *mm*)	0.024047	0.009576	0.006900	0.001073	0.001068
Tracking error (RMS, *mm*)	0.165731	0.196732	0.181819	0.146752	0.001694

Downloaded From: http://dynamicsystems.asmedigitalcollection.asme.org/ on 04/27/2014 Terms of Use: http://asme.org/terms

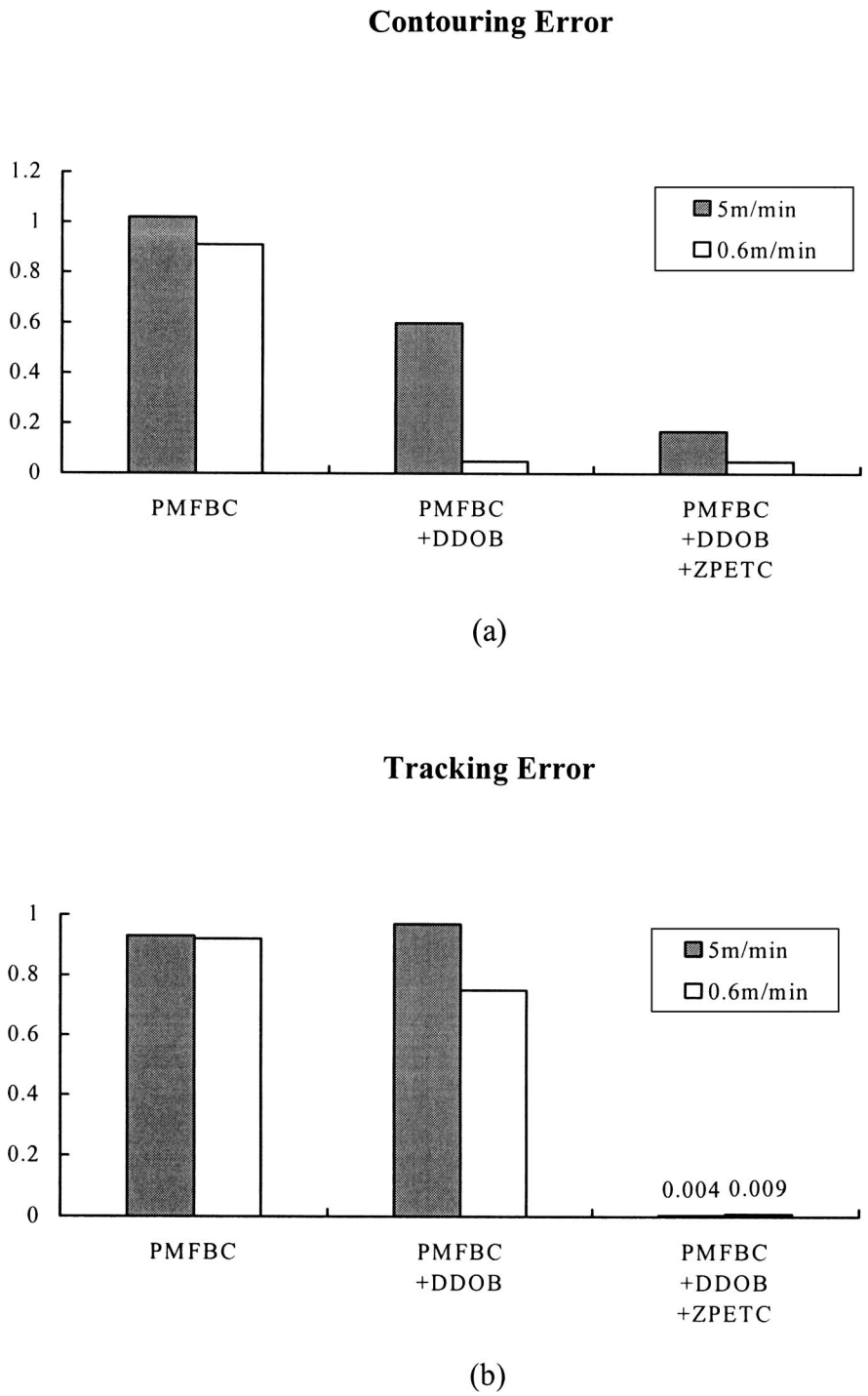

Fig. 17 Normalized errors for circular commands

responses for all axes within a higher frequency range compared to matched dc-gain control. Therefore, experimental results of PMFBC also lead to meaningful reduction of contouring accuracy in linear motion especially in the case of high-speed operation as in Tables 3 and 4 (case iv).

2. Note that the application of PMFBC (case iv) does not render satisfactory improvement in circular contouring as in Tables 1 and 2. Figure 13 shows that the nonlinear slip-stick phenomenon is still significant, because PMFBC is mainly a linear model-based control design. By introducing the DDOB to compensate for the undesirable properties, results as shown in Tables 1 and 2 (case v) and Fig. 14 indicate that the contouring accuracy is then greatly improved, especially in the case of low-speed operation where the friction becomes more dominant.

3. Matched dc-gain control and PMFBC generally improves the contouring accuracy as in Tables 1–4 (case ii). However, their tracking accuracy is merely improved. By including the feedforward control ZPETC in the proposed PMFBC structure, both the tracking error and contouring error are thus further reduced (case vi). Note that applications of the ZPETC only does not render improvement in contouring accuracy [13].

Downloaded From: http://dynamicsystems.asmedigitalcollection.asme.org/ on 04/27/2014 Terms of Use: http://asme.org/terms

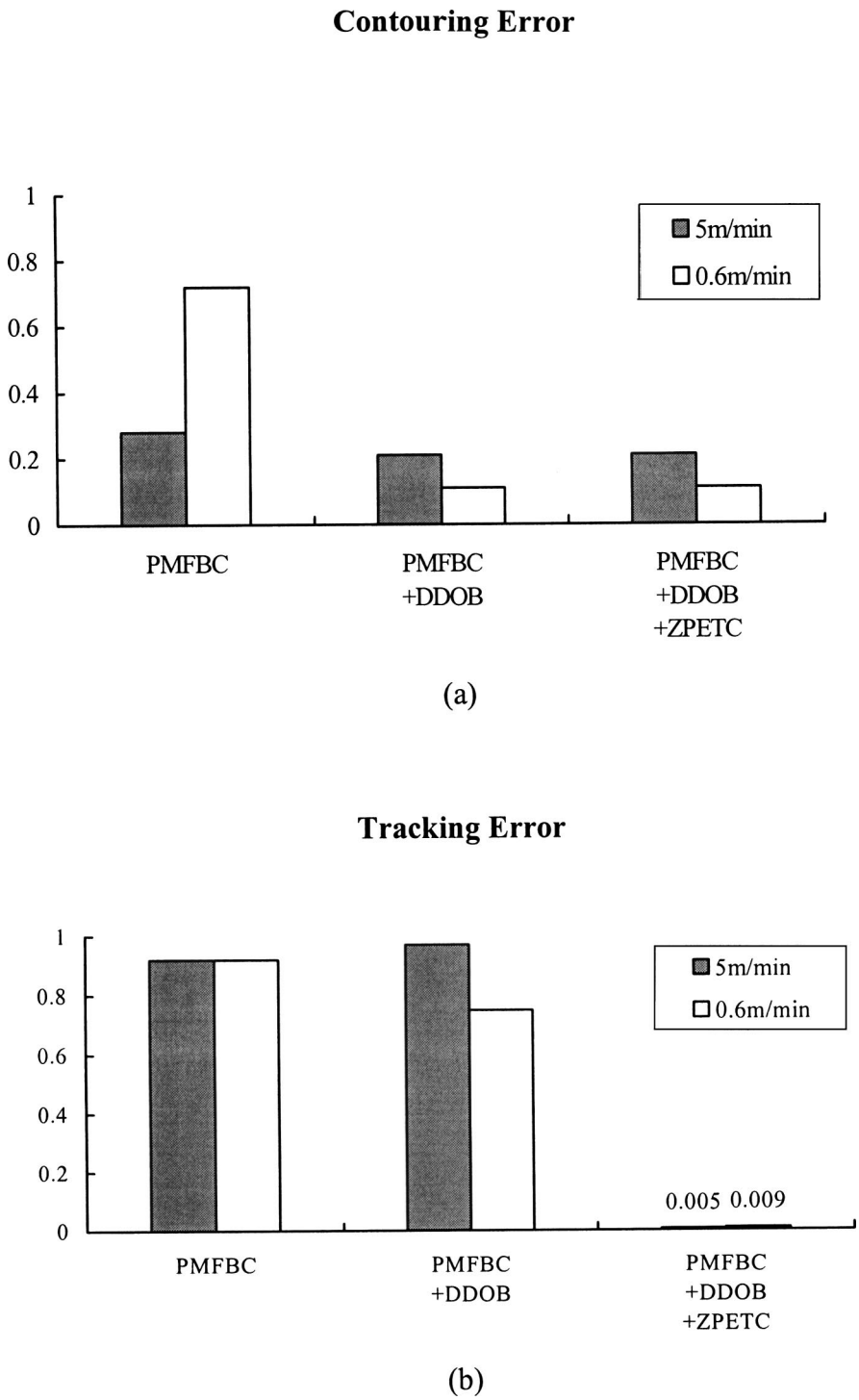

Fig. 18 Normalized errors for linear commands

6 Conclusion

In practice, mismatched frequency responses among axes seriously degrade contouring performance, especially under high-speed operations. The proposed PMFBC design leads to perfectly matched frequency responses among all axes and thereby achieves highly accurate contouring. Moreover, because the model-based PMFBC design is sensitive to nonlinearity, external disturbances, and plant uncertainty, a new DDOB was developed in this paper for nonminimum phase discrete-time systems. Furthermore, we have shown that the feedforward controller ZPETC can be directly applied to further reduce the tracking error. The feasibility of the present design has also been proven by using a reduced-order model. Experimental results on a CNC machining center show that the proposed control structure significantly improves both contouring and tracking performance for precise multi-axis motion systems under high-speed operations.

Acknowledgment

This work was supported by the National Science Council, Republic of China, under Contract No. NSC 89-2212-E-009-018.

Downloaded From: http://dynamicsystems.asmedigitalcollection.asme.org/ on 04/27/2014 Terms of Use: http://asme.org/terms

References

[1] Poo, A., Bollinger, J. G., and Younkin, W., 1972, ''Dynamic Error in Type Contouring Systems,'' IEEE Trans. Ind. Appl., **8**(4), pp. 477–484.

[2] Tomizuka, M., 1987, ''Zero Phase Error Tracking Algorithm for Digital Control,'' ASME J. Dyn. Syst., Meas., Control, **109**(**1**), pp. 65–68.

[3] Tsao, T. C., and Tomizuka, M., 1994, ''Robust Adaptive and Repetitive Digital Tracking Control and Application to A Hydraulic Servo for Noncircular Machining,'' ASME J. Dyn. Syst., Meas., Control, **116**(1), pp. 24–32.

[4] Xia, J. Z., and Menq, C. H., 1995, ''Precision Tracking Control of Nonminimum Phase Systems With Zero Phase Error,'' Int. J. Control, **61**(4), pp. 791–807.

[5] Yeh, S. S., and Hsu, P. L., 1999, ''An Optimal and Adaptive Design of the Feedforward Motion Controller,'' IEEE/ASME Trans. Mechatronics, **4**(4), pp. 428–439.

[6] Koren, Y., 1980, ''Cross-Coupled Biaxial Computer for Manufacturing Systems,'' ASME J. Dyn. Syst., Meas., Control, **102**(4), pp. 265–272.

[7] Kulkarni, P. K., and Srinivasan, K., 1990, ''Cross-Coupled Control of Biaxial Feed Drive Servomechaniasms,'' ASME J. Dyn. Syst., Meas., Control, **112**(2), pp. 225–232.

[8] Chuang, H. Y., and Liu, C. H., 1991, ''Cross-Coupled Adaptive Feedrate Control for Multiaxis Machine Tools,'' ASME Trans. J. Dyn. Syst., Meas., Control, **113**(3), pp. 451–457.

[9] Jee, S., and Koren, Y., 1995, ''A Self-Organizing Fuzzy Logic Control for Friction Compensation in Feed Drives,'' Proceedings 1995 ACC, Seattle, pp. 205–209.

[10] Lo, C. C., 1998, ''Three-Axis Contouring Control Based on a Trajectory Coordinate Basis,'' JSME Int. J., Ser. C, **41**(2), pp. 242–247.

[11] Chiu, G. T. C., and Tomizuka, M., 1995, ''Contouring Control of Machine Tool Feed Drive Systems: A Task Coordinate Frame Approach,'' ASME J. Dyn. Syst., Meas., Control, **117**(1), pp. 503–510.

[12] Cheng, C. C., Chen, C. Y., and Chiu, G. T. C., 2002, ''Predictive Control With Enhanced Robustness for Precision Positioning in Frictional Environment,'' IEEE/ASME Trans. Mechatronics, **7**(3), pp. 385–392.

[13] Yeh, S. S., and Hsu, P. L., 1999, ''Analysis and Design of the Integrated Controller for Precise Motion Systems,'' IEEE Trans. Control Syst. Technol., **7**(6), pp. 706–717.

[14] Endo, S., Tomizuka, M., and Hori, Y., 1993, ''Robust Digital Tracking Controller Design for High-Speed Positioning Systems,'' Proceedings 1993 ACC, San Francisco, pp. 2494–2498.

[15] Lee, H. S., and Tomizuka, M., 1996, ''Robust Motion Controller Design for High-Accuracy Positioning Systems,'' IEEE Trans. Ind. Electron., **43**(1), pp. 48–55.

[16] Kempf, C. J., and Kobayashi, S., 1999, ''Disturbance Observer and Feedforward Design for a High-Speed Direct-Drive Positioning Table,'' IEEE Trans. Control Syst. Technol., **7**(5), pp. 513–526.

[17] Astrom, K. J., Hagander, P., and Sternby, J., 1984, ''Zeros of Sampled Systems,'' Automatica, **20**(1), pp. 31–38.

[18] Clarke, D. W., 1984, ''Self Tuning Control of Nonminimum Phase Systems,'' Automatica, **20**(5), pp. 501–517.

[19] Samar, R., Postlethwaite, I., and Gu, D. W., 1995, ''Model Reduction With Balanced Realization,'' Int. J. Control, **62**(1), pp. 33–64.

[20] Yeh, S. S., and Hsu, P. L., 1999, ''Estimation of the Contouring Error Vector for the Cross-Coupled Control Design,'' IEEE/ASME Trans. Mechatronics, **7**(1), pp. 44–51.

Downloaded From: http://dynamicsystems.asmedigitalcollection.asme.org/ on 04/27/2014 Terms of Use: http://asme.org/terms